Design of a Reconfigurable Filtenna with Constant Bandwidth for Enhanced 5G mmWave Communication and Spectrum Coexistence

Shaghayegh Vosoughitabar

Electrical and Computer Engineering

Rutgers University

New Jersey, USA

sha.vosoughitabar@rutgers.edu

Narayan B. Mandayam

Electrical and Computer Engineering

Rutgers University

New Jersey, USA

narayan@winlab.rutgers.edu

Joseph F. Brodie *AKRF, Inc* Maryland, USA jbrodie@akrf.com

Behzad Golparvar
Civil and Environmental Engineering

Rutgers University
New Jersey, USA
behzad.golparvar@rutgers.edu

Ruo-Qian Wang

Civil and Environmental Engineering

Rutgers University

New Jersey, USA

rq.wang@rutgers.edu

Chung-Tse Michael Wu
Electrical and Computer Engineering
Rutgers University
New Jersey, USA
ctm.wu@rutgers.edu

Abstract—A reconfigurable substrate integrated waveguide (SIW) filtenna operating in the 5G millimeter Wave (mmWave) band is presented, where varactors are integrated into the filtering-antenna structure to change the resonant frequency and coupling between the SIW resonators. The proposed structure allows for the reconfigurability of the antenna radiation frequency band in the range of 24-27 GHz, covering most of the 3GPP n258 band, with a constant bandwidth of 400 MHz and broadside radiation pattern. A prototype of the proposed mmWave filtenna is designed and fabricated, where the measurement results are in good agreement with the simulation. The proposed cost-effective and scalable filtenna is an ideal candidate for deployment in 5G wireless networks, with the ability to reduce adjacent channel interference (ACI) and enable passive spectrum coexistence with weather sensors in the 23.8 GHz band.

 $\label{limit} \begin{array}{ll} \textit{Index Terms}{-}\mathsf{5G}, \, \mathsf{filtenna}, \, \mathsf{millimeter} \, \, \mathsf{wave} \, (\mathsf{mmWave}), \, \mathsf{passive} \, \\ \mathsf{spectrum} \, \, \, \mathsf{coexistence}, \, \, \mathsf{substrate} \, \, \, \mathsf{integrated} \, \, \, \mathsf{waveguide} \, \, \, (SIW), \, \\ \mathsf{tunable} \, \, \mathsf{filter} \, \, \, \\ \end{array}$

I. INTRODUCTION

The 5G New Radio (NR) is globally recognized as the advanced standard for 5G wireless air interfaces, operating on the frequency bands referred to as Frequency Range 1 (FR1) and Frequency Range 2 (FR2). FR2, in particular, operates within the millimeter-wave spectrum, covering a range from 24.25 GHz to 52.6 GHz. As the expansion of 5G wireless communication networks has surged in recent years, it has become crucial to address the issue of interference from 5G transmission networks with adjacent frequency bands. For instance, this coexistence challenge has drawn attention from various aviation associations, who have raised concerns that the public auctioning of the C-band spectrum (3.7 GHz - 4.2 GHz) within FR1 could cause harmful interference to

This work was supported by the National Science Foundation (NSF) under Grant SWIFT-2128077, ECCS-2028823 and ECCS-2229384.

radar altimeters used in all types of civil aircraft [1]–[3]. Such interference could lead to catastrophic outcomes, as it may result in the loss of radar altitude information or the production of inaccurate radar altitude data [4]. These concerns underscore the importance of carefully managing spectrum allocation and addressing potential interference to ensure the safety and reliability of critical aviation systems.

In the FR2 regime, deployment of spectrum above 24 GHz for 5G services, has raised considerable concerns regarding the accuracy of weather forecasting, performed by employing satellites sensing in the 23.8 GHz band [5], which is critical for weather predictions. As can be seen in Fig. 1, water vapor molecules absorb and then emit a fair amount of signal around 23.8 GHz and observations of this signal is a well-known method for remotely sensing the atmospheric water content, which is the driving force behind cloud formation and the development of storms. On the other hand, n258 band, as illustrated in Fig. 2, is designated for mmWave communication in 5G networks, covering frequencies from 24.25 GHz to 27.5 GHz with standard channel bandwidths of 50, 100, 200, and 400 MHz [6]. The out-of-band radiations from antennas incorporated in the 5G networks to send a desired signal in this band, interfere with the emitted signals from the earth and atmosphere which are measured by microwave radiometers installed on meteorological satellites, in the 23.8 GHz band.

Furthermore, it is anticipated that the spatial density of the 5G base stations will increase across the majority of the geographic regions in the future [7], [8]. As a result, the leakage of mmWave 5G signals into the 23.8 GHz band might cause errors in weather forecasting. Therefore, researchers have been increasingly focusing on investigating this interference, as highlighted in studies [9]–[13]. In this regard, the authors of a recently published article present an

inclusive research on the out-of-band interference, origina from realistic 5G mmWave infrastructures to weather satel sensing in the 23.8 GHz frequency band [12]. In this st the interference stemming from a single interferer as wel a network of interferers including Users and base stat located in New York City are modeled and investiga The results of this study show that aggregate interfere from a network of uplink or downlink interferers, given existing 5G network densities, would be detrimental in r atmospheric conditions. Subsequently, the authors endorse apprehensions regarding the spectrum coexistence between 5G mmWave networks and passive weather sensing thro microwave radiometers that have been expressed by me rological scientists and experts at the National Oceanic Atmospheric Administration (NOAA) [14]-[20]. In ano study [13], inaccuracies in temperature and rainfall predict are reported as a result of certain 5G mmWave leakage the 23.8 GHz band, by employing the Weather Research Forecasting Data Assimilation (WRFDA) model as a nur

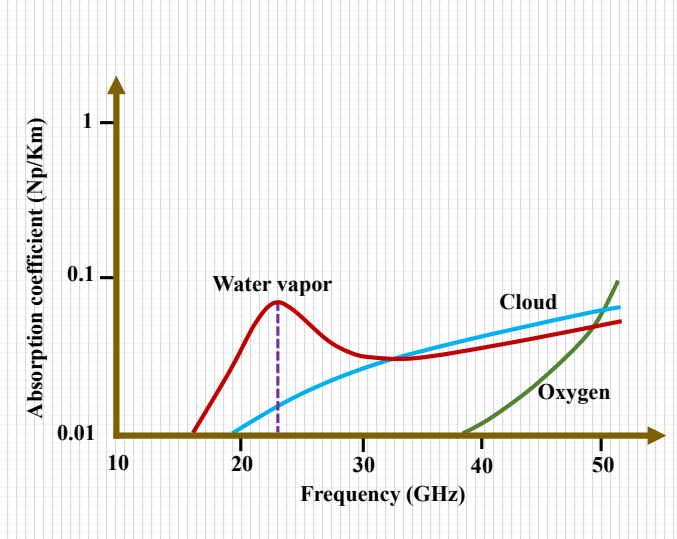


Fig. 1. Atmospheric absorption spectrum for typical conditions [22].

Taking into account the extensive research conducted over the past years, it is evident that more engineering solutions and regulatory policies are needed to curb the leakage from the n258 band into the 270 MHz bandwidth near the 23.8 GHz frequency. For instance, the work in [23] proposes a theoretical framework for 5G mmWave networks that includes using filtering antennas (filtennas) at the transmitter, combined with strategically allocating power and bandwidth. This approach is designed to meet system performance criteria while also reducing interference with the nearby weather sensing band.

The remainder of the paper is organized as follows. Section II describes the background of filtennas, operating in either FR1 or FR2 band. Section III elucidates the proposed reconfigurable filtenna design and its fabrication process. Section IV presents the simulation and measurement results, including the return loss (S_{11}) and radiation gain of the reconfigurable

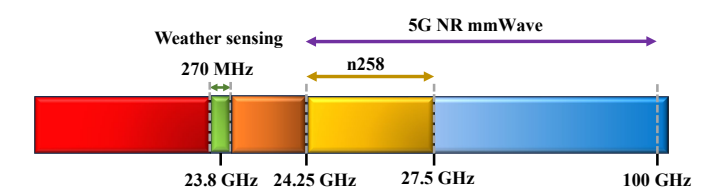


Fig. 2. 5G NR mmWave and weather sensing band around 23.8GHz.

II. BACKGROUND OF FILTERING ANTENNA (FILTENNA)

In recent years, design of tunable, reconfigurable, compact, and cost-effective components such as filters and antennas has attracted much attention [24]. In this context, a promising element for the design of 5G front-end devices is the filtering antenna, or filtenna, possessing characteristics such as effective out-of-band radiation suppression, seamless integration, and cost-effectiveness [25]–[30]. As mentioned earlier, n258 band covers frequencies from 24.25 GHz to 27.5 GHz, offering a maximum usable bandwidth of 400 MHz [6]. Therefore, ensuring flexibility to encompass this band while preserving a consistent radiation bandwidth is crucial for diverse 5G wireless communication systems.

To this end, a reconfigurable filtenna as a compact and multi-functional structure is a good candidate for achieving radiation tunability. Various configurations have been reported in the literature for designing tunable or reconfigurable filtennas. However, the majority of these operate within the FR1 band, specifically below 6 GHz. In [31], a varactor-based tunable filter is integrated into the feeding line of a printed Vivaldi antenna. In [32], a filtering stub is added to the feeding line of a quarter wave monopole antenna and PIN diodes are incorporated into the structure to make a tunable filtenna. An array of slotted rings embedded with varactors is placed on top of an ultra-wideband planar monopole antenna to realize a tunable filtenna in [33]. In [34], a reconfigurable filtenna using a double arm ring resonator operating in K/Ka band is designed by utilizing PIN diodes as tunable resistors. Although the radiation frequency can be changed in these designs, the radiation bandwidth of the filtenna is not fixed, which instead will increase as the frequency becomes higher. Such reconfigurable filtennas are not applicable to the scenarios where a constant radiation bandwidth is required. In [35], a reconfigurable filtering patch antenna operating from 2.05 to 2.52 GHz with frequency and bandwidth tunability is reported by utilizing an F-shaped probe. However, this design requires a complex non-planar feeding network, which may not be applicable for a filtenna operating in the mmWave band. In [25], a tunable filtenna with defected ground-plane structure (DGS) resonators in the mmWave band for 5G applications is reported. Nevertheless, the DGS topology may increase the back lobes, the design procedure is quite complex in this work, and the radiation bandwidth is not controllable by tuning the radiation frequency. On the other hand, substrate-integrated-waveguide (SIW) technology appears as a suitable platform for designing low loss and cost-effective filters and antennas with simple feeding network and good power handling capability in the mmWave regime [36], [37].

In this work, a mmWave tunable SIW filtenna incorporating varactor diodes as tuning elements is presented, in which the radiation bandwidth can remain constant (around 400 MHz) throughout the entire radiation frequency band. The schematic of the proposed reconfigurable filtenna is shown in Fig. 3, which can be applied in 5G wireless communication to transmit and receive the filtered-signal in a desired frequency band of 24 - 27 GHz, while decreasing the ACI into the neighboring 23.8 GHz band that is used by passive sensors (e.g. Advanced Microwave Sounding Unit (AMSU)-A sensors [38]) installed in weather observing satellites that dynamically monitor and measure the atmospheric radiance utilized to predict the density of water vapor in the atmosphere for weather forecasting [13], [23].

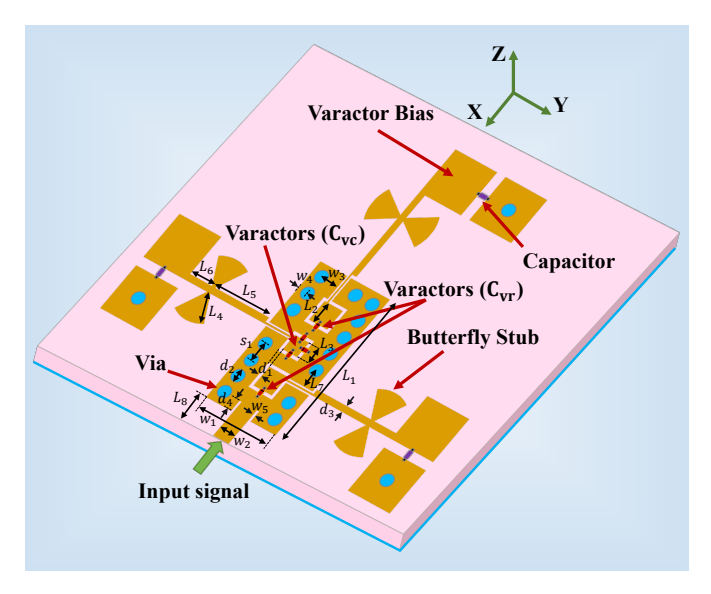


Fig. 3. Schematic of the proposed tunable filtenna. Dimensions (millimeter): $L_1=9.5,\,L_2=1.3,\,L_3=1,\,L_4=1.85,\,L_5=4,\,L_6=1.7,\,L_7=1.05,\,L_8=1.65,\,w_1=5,\,w_2=1.1,\,w_3=1.2,\,w_4=0.7,\,w_5=0.15,\,d_1=0.2,\,d_2=0.8,\,d_3=0.4,\,d_4=0.7,\,S_1=1.15.$

III. FILTENNA DESIGN AND FABRICATION

The design procedure begins with devising one square SIW cavity resonator. Utilizing the formula provided in (1) [39], the size of the cavity is determined to position the resonant frequency of the primary cavity mode (TE_{101}) above 30 GHz, accounting for the subsequent reduction in frequency due to varactor loading.

$$f_{101} = \frac{c_0\sqrt{2}}{2\sqrt{\epsilon_r}(a - \frac{d^2}{0.95p})},\tag{1}$$

where f_{101} represents the resonant frequency of the TE_{101} mode. a denotes the dimensions of the square cavity on a

substrate with a dielectric constant ϵ_r . d stands for the via hole diameter, and p signifies the center-to-center pitch between adjacent vias. Additionally, c_0 represents the speed of light. A square slot is created on top of the cavity serving as the radiating element. After that, a varactor is incorporated into the slot to vary the resonant frequency between 24 to 28 GHz. The electric (E)-field distribution is shown in Fig. 4, where the resonant frequency occurs at 25.4 GHz with a specific varactor value of 0.28 pF. As can be seen, by creating the square slot and integrating the varactor, the E-field distribution will be perturbed. Subsequently, two tunable cavity resonators are cascaded to form a filtenna. By changing the bias voltages of the integrated varactors, although the radiation frequency can be varied, the radiation bandwidth will also change, which may not be desirable in most of the wireless applications. Achieving radiation tunability with a constant bandwidth requires the coupling control between the two resonators, which is similar to the design of a tunable filter with a fixed bandwidth. To this end, the vias between the two SIW resonators are removed, whereas additional varactors are added to enable coupling tunability as shown in Fig. 3. For biasing the varactors, radial stubs are utilized to prevent the signal flow from the resonators to the DC bias pads in the frequency range of 24-27 GHz.

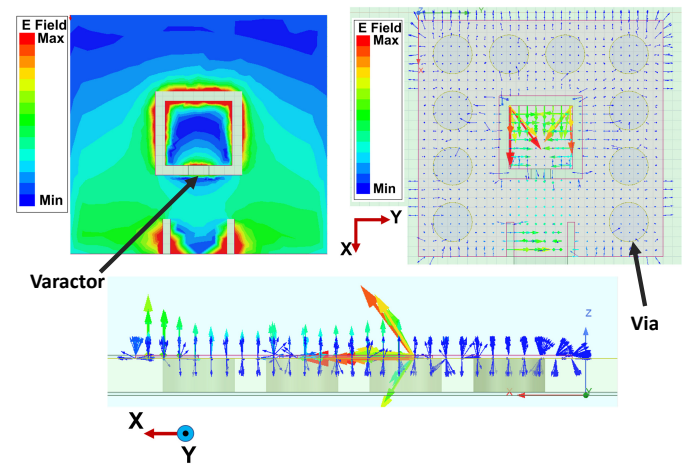


Fig. 4. Electric-field magnitude and vector of one single cavity resonator.

According to the filter synthesis approach [40], [41], the $(N+2) \times (N+2)$ immittance matrix [A] of an N^{th} order filter (The rows and columns are indexed as $S,1,2,\cdots,N,L$ where S and L refer to the source and load, respectively.) can be written as:

$$[A] = [M] + \lambda'[I] - j[R],$$
 (2)

where [M] is the coupling matrix, [I] is a diagonal matrix with $[I]_{SS} = [I]_{LL} = 0$, $[I]_{11} = [I]_{22} = \cdots = [I]_{NN} = 1$, where $[I]_{xy}$ is the (x,y) element of the matrix [I]. Moreover, [R] is the termination matrix whose elements are all zero, except $[R]_{SS} = [R]_{LL} = 1$, and λ' is defined as:

$$\lambda' = \frac{f_0}{BW} [(\frac{f}{f_0} - \frac{f_0}{f}) - j\frac{1}{Q_u}], \tag{3}$$

where f_0 is the center frequency, BW is the bandwidth of the filter, and Q_u is the unloaded quality factor of the resonators. Finally, the S-parameters of the filterna are obtained as [40]:

$$S_{11} = 1 + 2j[A^{-1}]_{SS}, \quad S_{21} = -2j[A^{-1}]_{LS},$$
 (4)

Fig. 5 depicts the coupling diagram of our proposed filtenna. The coupling between each resonator and the load is for modeling the radiation from the filtenna to the free space. Considering this, a second order Chebyshev filter with the center frequency of 25.4 GHz and fractional bandwidth of 1.5% is synthesized [42], and the corresponding coupling matrix M is shown in Fig. 5. The bias voltages of the varactors are adjusted to achieve the coupling matrix elements, following the methodology outlined in [43] for designing a microstrip filter using a full-wave simulator. The corresponding S-parameters based on (4) and simulation of the designed filtenna in HFSS are plotted in Fig. 6. As can be observed, within the radiation bandwidth, the simulated and theoretical frequency response are in great agreement. On the other hand, the differences outside of the radiation bandwidth may be due to the loading effect of the varactors, as well as the losses, resulting in decreasing the overall quality factors of the SIW resonators. It is noted that by tuning the varactors' bias voltages, the

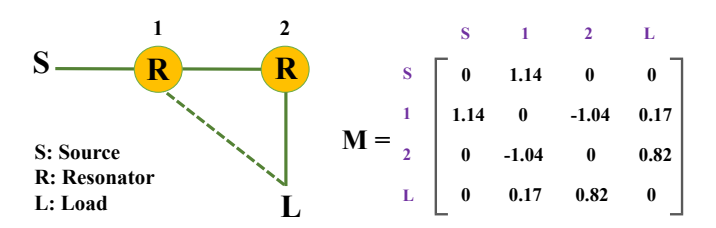


Fig. 5. The network coupling and corresponding coupling matrix.

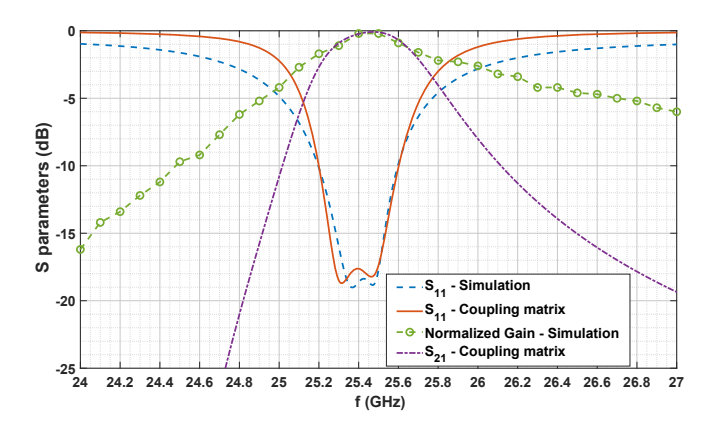


Fig. 6. Calculated S-parameters of the proposed filtenna based on the coupling matrix method and EM simulation.

IV. SIMULATION AND MEASUREMENT

In the EM simulation, each varactor is modeled with a series RC circuit, in which the values for R and C are obtained based on the model provided in the varactor datasheet under different bias voltages. The fabricated prototype is shown in Fig. 7, which is built on an RO5880 substrate with a thickness of 0.381 mm. Flip-chipped varactor diodes (MAVR-000120-141) from MACOM are employed, where the capacitance can be tuned from 0.18 pF to around 0.9 pF by changing the varactor bias voltages from 12 V to 1 V.

Fig. 8 plots the simulated and measured S_{11} under various varactor bias conditions. As one can clearly observe, the tunability of the center frequency along with an almost 400 MHz constant radiation bandwidth in the simulation agrees very well with the measurement results of the fabricated filtenna prototype. To validate the filtering behavior of the filtenna, Fig. 9 illustrates the comparison between measured and simulated gain versus frequency for varying bias voltages of the varactors. It can be seen that the out-of-band rejection is more effective in the lower frequency range due to the presence of a null resulting from the cross coupling between the first resonator and the load. This null can be strategically utilized to reduce the leaked power to the 23.8 GHz band utilized in weather observing.

The simulated and measured co-polarization and cross-polarization radiation patterns for different varactor bias voltages are also plotted in XZ and YZ planes in Fig. 10. The measured radiation gain of the proposed filtenna in the center frequency of each radiation bandwidth is around 4.2 dBi as can be seen in Fig. 10, which matches with the simulation result. Moreover, according to the full-wave simulation, the antenna efficiency is around 60%. The difference between the simulated and measured radiation patterns in the XZ plane may come from the asymmetric connector effects during the measurement.

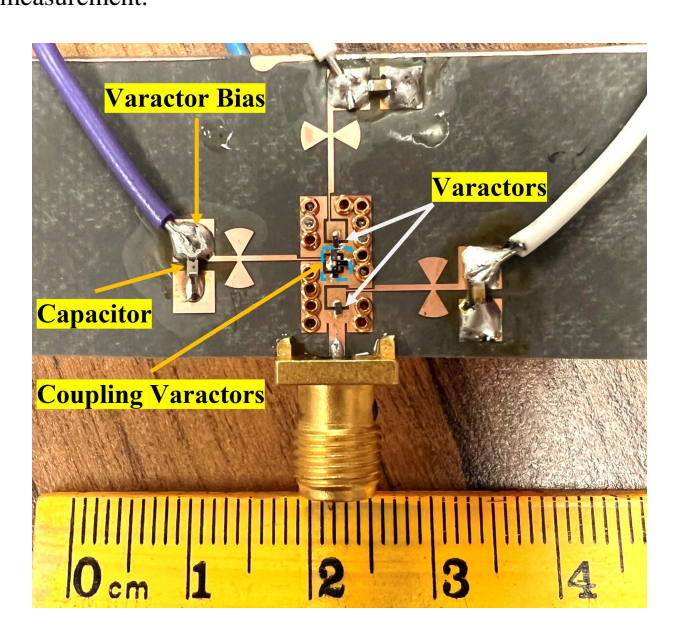


Fig. 7. Fabricated reconfigurable filtenna.

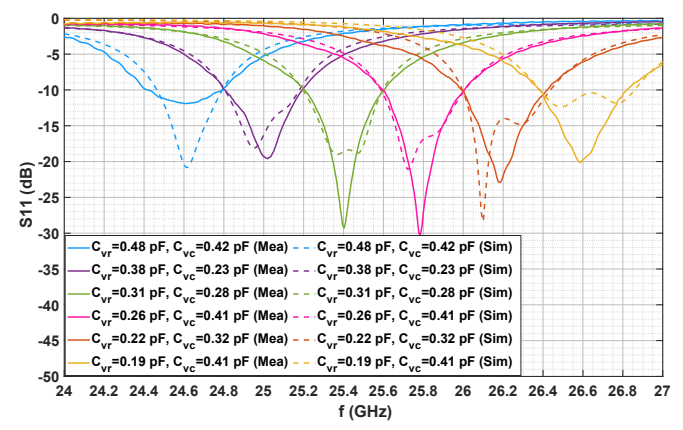


Fig. 8. Simulated and measured S_{11} of the filtenna for different bias voltages of the varactors.

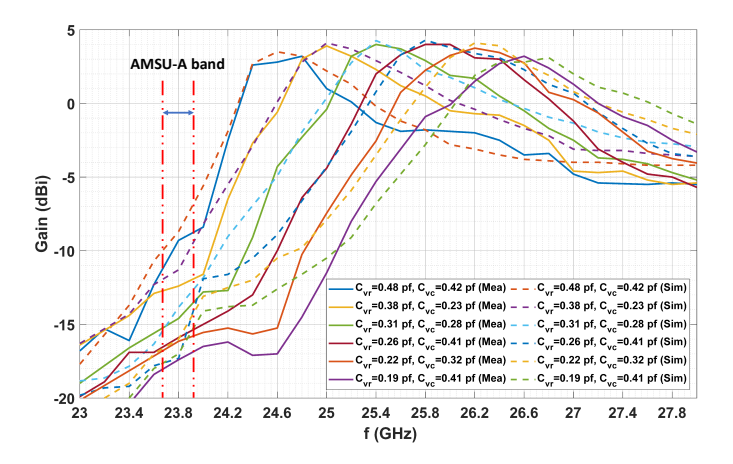


Fig. 9. Simulated and measured gain of the filtenna for different bias voltages of the varactors.

Table I compares the proposed reconfigurable filtenna with other related works reported in the literature. In [32], [34] while the filtennas are tunable, due to the use of PIN diodes, the tunability is discrete. As can be observed, in most of the reported works, varactors are integrated into the structure to provide continuous tunability. On the other hand, tunable filtennas in mmWave band are reported only in [25], [34]. However, in [34] only the simulation results are reported and there is no fabricated prototype with experimental validation. Furthermore, in both cases, while the radiation frequency is tunable, there is no control on the radiation bandwidth. To the contrary, for the reconfigurable filtenna proposed in this work, the bandwidth and radiation patterns can be kept almost unchanged when changing the radiation frequency.

It is worth noting that, according to the principle of filter design, increasing the filter order leads to a faster rolloff rate, as can be seen in Fig. 11 for an ideal Chebyshev filter response [44]. Akin to this principle, and given that plotting the gain of a filterna versus frequency resembles the frequency response of a filter, a high-order filtering antenna with more radiation/filtering elements through cascading more SIW resonators can achieve an even sharper out-of-band signal

rejection. However, this approach comes with a downside. Adding varactors to the filtenna allows for tuning its radiation band, but this also leads to increased power loss, especially when a greater number of varactor-integrated resonators are used. This increased power loss is due to the resistances introduced by the varactors, which result in greater power dissipation. Therefore, there is a trade-off between power efficiency and interference reduction in such designs. To optimize a high-order filtenna with strong out-of-band suppression, it is crucial to use varactors with very low resistances. We refer the reader to [23] where an integrated resource allocation approach that addresses the trade-off in power efficiency and leakage reduction is undertaken.

TABLE I

COMPARISON OF THE PROPOSED TUNABLE FILTENNA CHARACTERISTICS

WITH OTHER RELATED WORKS

Ref.	Topology	Tuning	Frequency	Bandwidth	Gain
		(C/D)*	band (GHz)	control	(dBi)
[31]	Printed	С	6.16 - 6.6	No	6
[32]	Etching slots	D	1.66 - 3.82	No	3
[33]	FSS	С	3.8 - 4.4	No	3
[34]	Stack	D	23.75 - 29.5	No	13
[35]	Patch	С	2.05 - 2.52	Yes	8
[25]	DGS	С	25 - 28.5	No	9
[45]	DGS	С	2.44 - 3.19	No	4
[46]	Patch	С	1.3 - 3	No	5
This	SIW	С	24.4 - 26.8	Yes	4.2
work	5111		24.4 - 20.0	165	-±.2

^{*} C: Continuous, D: Discrete

V. CONCLUSION AND FUTURE DIRECTIONS

A reconfigurable SIW filtenna in mmWave band was proposed. The radiation frequency can be tuned from 24 to 27 GHz, while maintaining a nearly constant radiation bandwidth of around 400 MHz. It is noted that the proposed configuration can also be potentially utilized for designing a reconfigurable filtenna with a narrower radiation bandwidth to accommodate standard channel bandwidths such as 100 and 200 MHz in the n258 band. As proof-of-concept, a prototype of the proposed filtenna was fabricated, and the measurement results including S_{11} , gain versus frequency, and radiation pattern agree well with the simulation results and theoretical prediction. The proposed filtenna may be used in wireless communication networks for 5G mmWave applications that demand spectral filtering radiation characteristics, which is particularly useful for passive spectrum coexistence with weather sensors. Beyond 5G mmWave, the design methodology presented here is

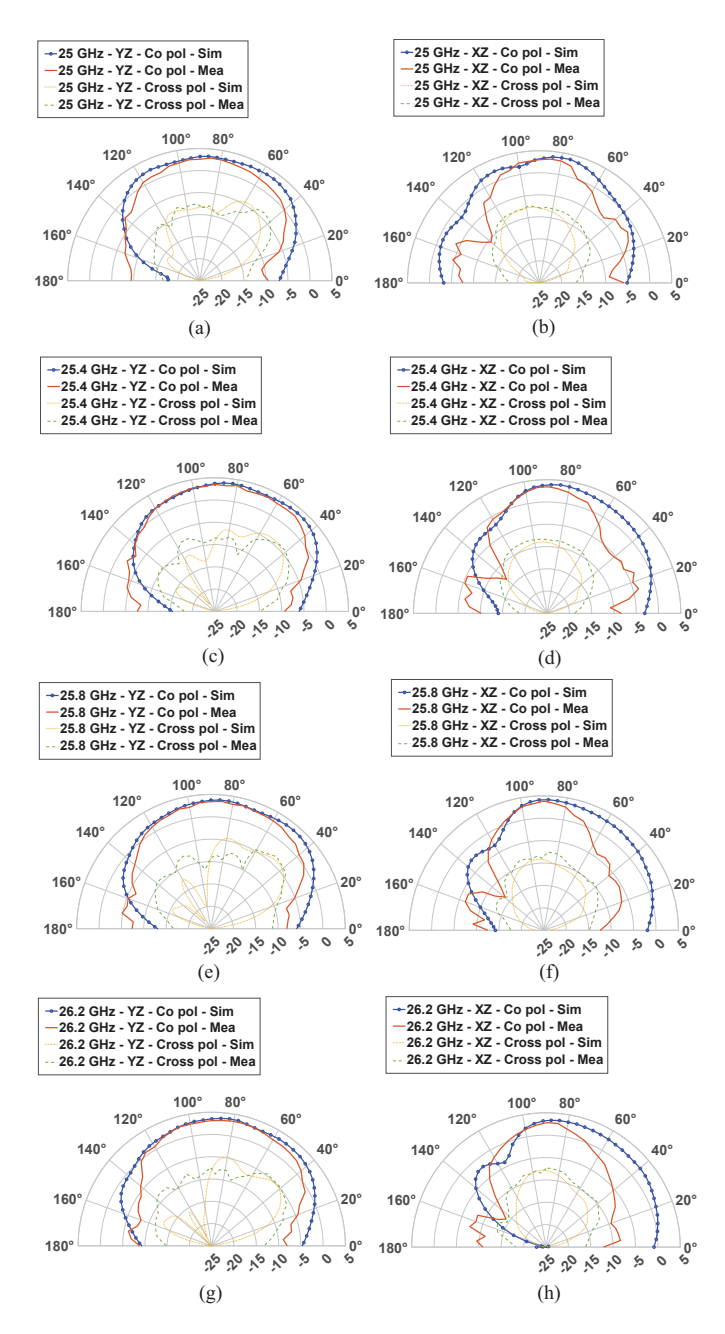


Fig. 10. Simulated and measured radiation patterns (dBi) for different varactor values. (a), (b) C_{vr} =0.38 pF, C_{vc} =0.23 pF. (c), (d) C_{vr} =0.31 pF, C_{vc} =0.28 pF. (e), (f) C_{vr} =0.26 pF, C_{vc} =0.41 pF. (g), (h) C_{vr} =0.22 pF, C_{vc} =0.32 pF.

capable of addressing emerging spectrum coexistence challenges in other bands. The dimensions of the filtenna can be modified to operate in other frequency bands such as FR1 as well as the proposed new spectrum allocations in FR3 [47], [48], and used to address the mitigation of out-of-band emissions for enabling both passive and active spectrum coexistence in these bands.

REFERENCES

[1] I. C. A. O. (ICAO), "5G interference with radar altimeter frequency band," Nov 2020. [Online]. Available: https://www.icao.int/safety/FSMP/MeetingDocs/Forms/AllItems.aspx

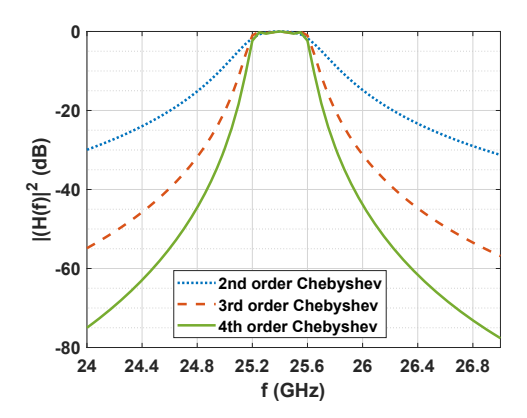


Fig. 11. Frequency response of the Chebyshev filter with center frequency of 25.4 GHz and bandwidth of 400 MHz for different orders.

- [2] K. Reichmann, "Will the 5G fast plan lead to spectrum issues for aircraft?" Jan 2021. [Online]. Available: https://www.aviationtoday.com/2021/01/18/will-5g-fast-plan-lead-spectrum-issues-aircraft.
- [3] M. Solkin, "Electromagnetic interference hazards in flight and the 5G mobile phone: review of critical issues in aviation security," *Transportation research procedia*, vol. 59, pp. 310–318, 2021.
- [4] A. L. P. A. (ALPA), "Aircraft operations and radar altimeter interference from 5G," Jun 2023. [Online]. Available: https://www.alpa.org/resources/aircraft-operations-radar-altimeterinterference-5G.
- [5] Q. Liu, C. Cao, C. Grassotti, and Y.-K. Lee, "How can microwave observations at 23.8 ghz help in acquiring water vapor in the atmosphere over land?" *Remote Sensing*, vol. 13, no. 3, p. 489, 2021.
- [6] "5G NR Radios for Fifth Generation Networks." [Online]. Available: https://www.5gradio.com/5g-technology/5g-nr-frequency-bands.
- [7] B. Golparvar, S. Vosoughitabar, I. B. Majumdar, J. F. Brodie, N. Mandayam, C.-T. M. Wu, and R.-Q. Wang, "Impact of future spatio-temporal 5g leakage on weather forecasting accuracy," in 103rd AMS Annual Meeting - Poster presentation. AMS, 2023.
- [8] B. Golparvar, I. B. Majumdar, S. Vosoughitabar, J. F. Brodie, N. Mandayam, C.-T. M. Wu, and R. Wang, "A study on the impact of non-uniform 5g leakage on the accuracy of weather forecasts," in AGU Fall Meeting Abstracts, vol. 2022, 2022, p. 5.
- [9] Y. Cho, H.-K. Kim, M. Nekovee, and H.-S. Jo, "Coexistence of 5g with satellite services in the millimeter-wave band," *IEEE Access*, vol. 8, pp. 163 618–163 636, 2020.
- [10] T. Caillet, "Compatibility between eess (passive) in band 23.6–24 ghz and 5g in band 24.25–27.5 ghz," *Comptes Rendus. Physique*, vol. 22, no. S1, pp. 83–93, 2021.
- [11] E. Murakami, A. Linhares, L. C. Trintinalia, and L. C. Alexandre, "Coexistence between imt-2020 and eess(passive) in the 24 ghz band," in 2021 SBMO/IEEE MTT-S International Microwave and Optoelectronics Conference (IMOC), 2021, pp. 1–3.
- [12] A. Palade, A. M. Voicu, P. Mähönen, and L. Simić, "Will emerging millimeter-wave cellular networks cause harmful interference to weather satellites?" *IEEE Transactions on Cognitive Communications and Net*working, pp. 1–1, 2023.
- [13] M. Yousefvand, C.-T. M. Wu, R.-Q. Wang, J. Brodie, and N. Mandayam, "Modeling the impact of 5G leakage on weather prediction," in 2020 IEEE 3rd 5G World Forum (5GWF), 2020, pp. 291–296.
- [14] S. Hollister, "5G could mean less time to flee a deadly hurricane, heads of NASA and NOAA warn," May 2019. [Online]. Available: https://www.theverge.com/2019/5/23/18637356/5g-interfereweather-forecast-24ghz-frequency-band-satellite-predict-hurricane.
- [15] S. E. Benish, G. H. Reid, A. Deshpande, S. Ravan, and R. Lamb, "The impact of emerging 5G technology on us weather prediction," *Journal* of Science Policy & Governance, vol. 17, no. 2, 2020.
- [16] A. Witze, "Global 5G wireless deal threatens weather forecasts," Nov 2019. [Online]. Available: https://www.nature.com/articles/d41586-019-03609.

- [17] K. Chamberlain, "NOAA chief warns 24 GHz 5G would hamper weather forecasting," May 2019. [Online]. Available: https://www.fiercewireless.com/5g/noaa-chief-warns-24-ghz-5g-would-hamper-weather-forecasts
- [18] J. Brodkin, "5G likely to mess with weather fore-casts, but FCC auctions spectrum anyway," May 2019. [Online]. Available: https://arstechnica.com/tech-policy/2019/05/5g-networks-will-likely-interfere-with-us-weather-satellites-navy-warns/
- [19] D. Hosansky, "5G wireless networks threaten weather forecasts," July 2021. [Online]. Available: https://news.ucar.edu/132801/5g-wirelessnetworks-threaten-weather-forecasts-ncar-expert-tells-congress
- [20] M. J. Marcus, "5g/weather satellite 24 ghz spectrum disagreement: Anatomy of a spectrum policy issue," *IEEE Wireless Communications*, vol. 26, no. 4, pp. 2–3, 2019.
- [21] W. C. Skamarock, J. B. Klemp, J. Dudhia, D. O. Gill, Z. Liu, J. Berner, W. Wang, J. Powers, M. Duda, D. Barker et al., "A description of the advanced research WRF model version 4," NCAR tech. note ncar/tn-556+ str, vol. 145, 2019.
- [22] T. J. Hewison, "1D-VAR retrieval of temperature and humidity profiles from a ground-based microwave radiometer," *IEEE Transactions on Geoscience and Remote Sensing*, vol. 45, no. 7, pp. 2163–2168, 2007.
- [23] I. B. Majumdar, S. Vosoughitabar, C.-T. Michael Wu, N. B. Mandayam, J. F. Brodie, B. Golparvar, and R.-Q. Wang, "Resource allocation using filtennas in the presence of leakage," in 2022 IEEE Future Networks World Forum (FNWF), 2022, pp. 591–596.
- [24] Y. Tu, Y. I. Al-Yasir, N. Ojaroudi Parchin, A. M. Abdulkhaleq, and R. A. Abd-Alhameed, "A survey on reconfigurable microstrip filter–antenna integration: Recent developments and challenges," *Electronics*, vol. 9, no. 8, p. 1249, 2020.
- [25] K. R. Mahmoud and A. M. Montaser, "Design of compact mm-wave tunable filtenna using capacitor loaded trapezoid slots in ground plane for 5G router applications," *IEEE Access*, vol. 8, pp. 27715–27723, 2020.
- [26] A. K. Gangwar, M. S. Alam, V. Rajpoot, and A. K. Ojha, "Filtering antennas: A technical review," *International Journal of RF and Microwave Computer-Aided Engineering*, vol. 31, no. 10, p. e22797, 2021.
- [27] R. Lu, C. Yu, F. Wu, Z. Yu, L. Zhu, J. Zhou, P. Yan, and W. Hong, "Siw cavity-fed filtennas for 5g millimeter-wave applications," *IEEE Transactions on Antennas and Propagation*, vol. 69, no. 9, pp. 5269–5277, 2021.
- [28] R. Lu, C. Yu, Y. Zhu, X. Xia, and W. Hong, "Millimeter-wave dual-band dual-polarized siw cavity-fed filtenna for 5g applications," *IEEE Transactions on Antennas and Propagation*, vol. 70, no. 11, pp. 10104–10112, 2022.
- [29] M.-C. Tang, D. Li, X. Chen, Y. Wang, K. Hu, and R. W. Ziolkowski, "Compact, wideband, planar filtenna with reconfigurable tri-polarization diversity," *IEEE Transactions on Antennas and Propagation*, vol. 67, no. 8, pp. 5689–5694, 2019.
- [30] K.-Z. Hu, M.-C. Tang, M. Li, and R. W. Ziolkowski, "Compact, low-profile, bandwidth-enhanced substrate integrated waveguide filtenna," *IEEE Antennas and Wireless Propagation Letters*, vol. 17, no. 8, pp. 1552–1556, 2018.
- [31] Y. Tawk, J. Costantine, and C. G. Christodoulou, "A varactor-based reconfigurable filtenna," *IEEE Antennas and Wireless Propagation Letters*, vol. 11, pp. 716–719, 2012.
- [32] W. A. Awan, N. Hussain, S. Kim, and N. Kim, "A frequency-reconfigurable filtenna for GSM, 4G-LTE, ISM, and 5G sub-6 GHz band applications," *Sensors*, vol. 22, no. 15, p. 5558, 2022.
- [33] J. L. Durbin and M. A. Saed, "Tunable filtenna using varactor tuned rings fed with an ultra wideband antenna," *Progress in Electromagnetics Research Letters*, vol. 29, pp. 43–50, 2012.
- [34] M. Patriotis, F. Ayoub, C. G. Christodoulou, and M. T. Chryssomallis, "A reconfigurable k/ka band filtenna using a double arm ring resonator," in 2019 IEEE International Symposium on Antennas and Propagation and USNC-URSI Radio Science Meeting, 2019, pp. 1479–1480.
- [35] P. F. Hu, Y. M. Pan, X. Y. Zhang, and B.-J. Hu, "A filtering patch antenna with reconfigurable frequency and bandwidth using f-shaped probe," *IEEE Transactions on Antennas and Propagation*, vol. 67, no. 1, pp. 121–130, 2019.
- [36] K. Nouri, T. H. C. Bouazza, B. S. Bouazza, M. Damou, K. Becharef, and S. Seghier, "Design of substrate integrated waveguide multi-band slots array antennas," *International Journal of Information and Electronics Engineering*, vol. 6, no. 4, pp. 221–225, 2016.

- [37] C.-T. M. Wu and T. Itoh, "An X-band dual-mode antenna using substrate integrated waveguide cavity for simultaneous satellite and terrestrial links," in 2014 Asia-Pacific Microwave Conference, 2014, pp. 726–728.
- 38] "AMSU-A." [Online]. Available: https://space.oscar.wmo.int/instruments/view/amsu-a.
- [39] Y. Cassivi, L. Perregrini, P. Arcioni, M. Bressan, K. Wu, and G. Conciauro, "Dispersion characteristics of substrate integrated rectangular waveguide," *IEEE Microwave and Wireless Components Letters*, vol. 12, no. 9, pp. 333–335, 2002.
- [40] R. J. Cameron, C. M. Kudsia, and R. R. Mansour, Microwave filters for communication systems: fundamentals, design, and applications. John Wiley & Sons, 2018.
- [41] S. Amari, U. Rosenberg, and J. Bornemann, "Adaptive synthesis and design of resonator filters with source/load-multiresonator coupling," *IEEE Transactions on Microwave Theory and Techniques*, vol. 50, no. 8, pp. 1969–1978, 2002.
- [42] R. Cameron, "General coupling matrix synthesis methods for chebyshev filtering functions," *IEEE Transactions on Microwave Theory and Techniques*, vol. 47, no. 4, pp. 433–442, 1999.
- [43] J.-S. G. Hong and M. J. Lancaster, Microstrip filters for RF/microwave applications. John Wiley & Sons, 2004.
- [44] D. Pozar, Microwave Engineering. Wiley, 2011.
- [45] Z. Wen, M.-C. Tang, and R. W. Ziolkowski, "Band-and frequency-reconfigurable circularly polarised filtenna for cognitive radio applications," *IET Microwaves, Antennas & Propagation*, vol. 13, no. 7, pp. 1003–1008, 2019.
- [46] M. A. Abdelghany, W. A. Ali, H. A. Mohamed, and A. A. Ibrahim, "Filtenna with frequency reconfigurable operation for cognitive radio and wireless applications," *Micromachines*, vol. 14, no. 1, p. 160, 2023.
- [47] Z. Hassan, E. Heeren-Moon, J. Sabzehali, V. K. Shah, C. Dietrich, J. H. Reed, and E. W. Burger, "Spectrum sharing of the 12 ghz band with two-way terrestrial 5g mobile services: Motivations, challenges, and research road map," *IEEE Communications Magazine*, pp. 1–7, 2023.
- [48] M. Ghosh, "Mid-band spectrum allocation challenges and options: licensed, unlicensed and shared," in NSF Spectrum Week, April 2023.